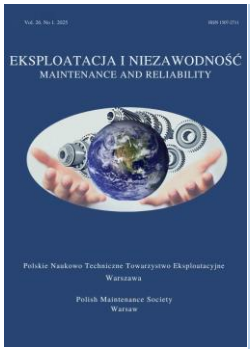

Eksploatacja i Niezawodnosc – Maintenance and Reliability
Volume 27 (2025), Issue 1
journal homepage: http://www.ein.org.pl

Article citation info:
Ma Q, Long J, Shi X, Liu Z, Guo Y, Temporal Constrained Dynamic Uncertain Causality Graph for Root Cause Analysis of Intermittent Faults, Eksploatacja i Niezawodnosc – Maintenance and Reliability 2025: 27(1) http://doi.org/10.17531/ein/192169

Temporal Constrained Dynamic Uncertain Causality Graph for Root Cause Analysis of Intermittent Faults

Indexed by: Web of Science Group

Qiqi Ma[a], Jiang Long[a], Xiangnan Shi[b], Zun Liu[a], Yangming Guo[c,*]

[a] The School of Computer Science, Northwestern Polytechnical University, China
[b] The Unmanned System Research Institute, Northwestern Polytechnical University, China
[c] The School of Cybersecurity, Northwestern Polytechnical University, China

Highlights

- A better understanding of the intermittency of fault symptoms from the perspective of temporal and state coupling between variables.
- A novel causal model, TC-DUCG, designed for analyzing intermittent faults caused by temporal and state coupling during fault propagation.
- A fault diagnosis inference method that takes into account the dynamic evolution of faults and the random uncertainty of the propagation process.

Abstract

The diagnosis of intermittent faults is crucial in the field of maintenance support. Unfortunately, most existing studies focus on the analysis of intermittent faults in single components, ignoring the more complex intermittent failures of equipment functions caused by the coupling of multivariate anomalous states in the fault propagation process. Existing diagnostic methods based on fault propagation models, which mainly focus on one-dimensional temporal or logical relationships, fall short in representing and reasoning about intermittent faults caused by temporal and state coupling. In this paper, a Temporal Constrained Dynamic Uncertain Causality Graph (TC-DUCG) model is developed to fill this gap and effectively model intermittent faults. Our model not only considers the probability of fault propagation among variables but also integrates temporal constraints. It also presents a diagnostic reasoning process to investigate potential causes of intermittent faults. An illustrative example is proposed to demonstrate the effectiveness of the proposed method in diagnosing intermittent faults.

Keywords
modeling intermittent fault, fault diagnosis and reasoning, TC-DUCG, temporal and state coupling

1. Introduction

Intermittent faults, also known as sporadic faults, exhibit a transient nature, lasting for a limited period before vanishing unpredictably [1]. Their intricate patterns pose challenges in conducting fault analysis, tracing the root causes, and promptly identifying fault locations. These faults can lead to resource wastage, reduced equipment availability, increased maintenance costs, and potential safety hazards in certain cases [2]. Owing to the characteristics of intermittent faults, they have attracted considerable attention in the field of maintenance support. Some effective intermittent fault diagnosis methods have been presented, as seen in references [3-9].

While numerous methods have been proposed for diagnosing intermittent faults [10], it is worth noting that most existing research primarily focuses on analyzing intermittent faults in individual components. Nevertheless, the actual intermittent fault process is often more complex. In practice,

(*) Corresponding author.
E-mail addresses: Q. Ma (ORCID: 0009-0000-3177-9051) mqq@mail.nwpu.edu.cn, J. Long (ORCID: 0000-0002-5805-6811) jlong@nwpu.edu.cn, X. Shi shixiangnan@mail.nwpu.edu.cn, Z. Liu (ORCID: 0000-0002-0617-7902) liuzun@nwpu.edu.cn, Y. Guo (ORCID: 0009-0001-5095-5206) yangming_g@nwpu.edu.cn,

intermittent faults in devices can be caused by the coupling of abnormalities in multiple variables.

Faults exhibit propagation characteristics and can impact multiple variables [11]. The manner in which faults propagate can be represented by the dependencies among these variables in a diagnostic model. These dependencies can take the form of either temporal or logical relationships [12]. Different combinations of variable states can lead to different fault symptoms. Owing to the dynamic evolution of faults and the random uncertainty in the fault propagation process, the symptoms of faults can be intermittent, occurring only when specific combined conditions of variables (both temporal and state coupling) are met. Therefore, it is crucial to accurately model the fault propagation process according to these characteristics and to comprehensively analyze the temporal and logical coupling mechanisms among variables during propagation. These steps are useful for gaining a deeper understanding of how faults propagate and manifest as intermittent symptoms.

A fault propagation model typically involves three essential steps: constructing a propagation model framework based on the qualitative dependencies between fault events; assigning numerical parameters to represent the characteristics of these fault events; and performing quantitative reasoning to diagnose the root cause responsible for the observed symptoms [13]. Fault Tree Analysis (FTA) is a widely used qualitative method for fault propagation modeling and diagnosis [14]. A fault tree describes the logical relationships between different fault events within a system. As discussed in [15], dynamic fault tree (DFT) analysis has been enhanced to account for dynamic behaviors, including sequence-dependent, functional-dependent, and priority relationships among failures. The authors proposed a stochastic computational approach for efficiently analyzing the failure probability of the top event in a DFT that includes priority AND (PAND) gates. Furthermore, stochastic models have been developed for the efficient analysis of spare gates and probabilistic common cause failures (PCCFs) in DFTs [16]. While methods based on fault tree analysis are primarily used in binary state systems with clear logical relationships. Difficulties in representing the uncertainty of fault relationships and multi-states limit the further application of such methods. Bayesian Network (BN) [17-18] is another commonly used technique in fault propagation modeling. It is a directed graphical model that can represent a set of random variables and their causal relationships. In reference [19], a BN-K2-EM approach is proposed to quantify the intensity of coupling influences among operational failures and to identify the failure propagation chains in accidents.

Nevertheless, reference [20] has indicated that the compact representation and inference capabilities of the BN model may not be well-suited for multivalued cases. To address this issue, Zhang et al. [21] proposed the Dynamic Uncertain Causality Graph (DUCG) for diagnosing faults in large and complex systems. The DUCG can compactly represent complex conditional probability distributions and incorporates logic gates to express intricate logical dependencies (state coupling) between variables. The DUCG model has been successfully applied to root cause diagnosis in various fields, including aluminum electrolysis systems [22], nuclear systems [23], and clinical diagnosis [24]. However, the DUCG model does not account for the temporal aspects of fault propagation, such as the duration of states and bounded fault propagation delays. Consequently, it is unable to model temporal dependencies between variables during fault propagation. To address this limitation, the Cubic DUCG was proposed, effectively modeling causal-temporal dependency relationships [23]. It should be noted that the Cubic DUCG does not consider time constraints in fault propagation. Furthermore, the model inference process does not account for the dynamic changes in fault source states or the presence of multiple fault sources.

It is important to note that several diagnostic models specifically address temporal information and can effectively model temporal dependencies between variables. One such model is the widely-used Timed Failure Propagation Graph (TFPG) model [25], which captures the temporal aspects of fault propagation in systems. However, the TFPG model assumes that the state remains unchanged after a fault effect reaches a node, which means it does not account for intermittent faults. Additionally, the causal relationships between variables in the TFPG model are deterministic, limiting its ability to effectively express the uncertainty in fault propagation.

It is evident that the DUCG model emphasizes the representation of uncertain causality, allowing it to express complex logical dependencies. On the other hand, the TFPG

model focuses on processing temporal information, enabling it to represent general forms of temporal dependency. In summary, both DUCG and TFPG have advantages in expressing dependencies during fault propagation. However, neither diagnostic model is capable of modeling intermittent faults caused by the coupling of temporal and state factors. To address the limitations of both the DUCG and TFPG models, this paper proposes a Temporal Constrained Dynamic Uncertain Causality Graph (TC-DUCG) model, which can flexibly represent the complex mechanisms underlying intermittent faults. A comparison of the modeling and reasoning properties of DUCG, TFPG, and TC-DUCG is presented in Table 1.

In this paper, we aim to gain a deeper understanding of the intermittency of fault symptoms from the perspective of temporal and state coupling among variables. The corresponding diagnostic reasoning process is also provided. This study considers that the states of system variables change dynamically during the occurrence, propagation, and evolution of faults. The causal relationships between variables are complex and uncertain. To express these dynamic and uncertain causal relationships between variables more intuitively and flexibly, the observation interval division criteria are applied to segment the evidence.

The main contributions of this paper are summarized as follows.

1) To analyze intermittent faults caused by temporal and state coupling during fault propagation, this paper proposes a novel causal model, TC-DUCG. The proposed model can flexibly represent the temporal and logical dependencies between multi-state variables with complex forms, accommodating scenarios where the state of a variable changes dynamically.
2) By considering the dynamic evolution of faults and the inherent uncertainty in the propagation process, a fault diagnosis inference method is proposed, aiming to accurately identify the root cause of intermittent faults. In this inference process, observation interval division criteria are applied to segment the evidence, and time range and logical match analysis of the evidence within the same time slice are performed to eliminate false alarms, thereby improving diagnostic accuracy.

This paper is organized as follows. After the introduction in Section 1, the preliminaries are presented in Section 2. Section 3 introduces the proposed TC-DUCG model. In Section 4, an illustrative example is provided to demonstrate the effectiveness of the TC-DUCG model in diagnosing intermittent faults. Finally, Section 5 concludes the paper.

2. Preliminaries

A. Fault Description

According to the IEEE Standards [26], an intermittent fault is defined as a fault that recurs frequently due to the same cause, persists for a limited period of time, and then disappears without any external corrective action, allowing the system to recover its ability to perform the required function. Generally, the occurrence and disappearance of intermittent faults are stochastic. A general representation of an intermittent fault is shown in Fig. 1.

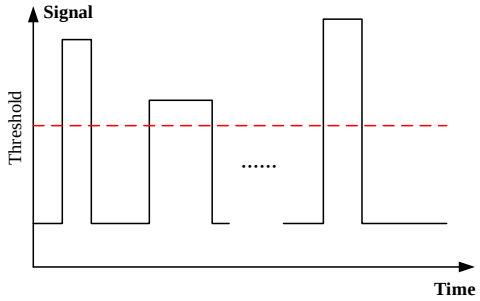

Fig. 1. A general representation of an intermittent fault.

Existing research on the mechanisms of intermittent faults primarily focuses on internal damage to individual device components, such as corrosion, wear, loose connections, and solder joint cracks [1]. Nevertheless, this approach may not accurately represent real-world intermittent fault scenarios. In practice, intermittent fault symptoms may be caused by the coupling of anomalies across multiple variables.

In this paper, intermittent faults are defined as instances where complex equipment fails to perform its specified function due to the coupling of system variables in both temporal and state domains. In practical applications, there may be intricate causal relationships among events (variables), and the coupling relationships across temporal and state dimensions can be diverse. Temporal information includes the timing of variable state changes, the duration of these states, and the sequence and intervals between multiple state changes. Multi-state information encompasses various fault levels, multiple degraded states of components, and a range of abnormal

Table 1. A comparison of the modeling and reasoning properties of DUCG, TFPG, and TC-DUCG.

Model	DUCG	TFPG	TC-DUCG
Propagation probability	Yes	No	Yes
Temporal constraints	No	Yes	Yes
Reasoning approach	Logical-based	Consistency-based	Based on logic and timing consistency
State can change	Yes	No	Yes
State of variable	Multi-state	Two-state	Multi-state
Logical relation	Combinational	OR/AND	Combinational

observation states (e.g., exceeding or falling below normal threshold ranges). Fault symptoms manifest only when variables meet certain combination conditions, involving both temporal and state coupling. For example, consider a scenario where the state condition requires that variable X_1 is in state α, and variable X_2 is in state β. The temporal condition specifies that state α must occur first and persist for at least t_1 before variable X_2 transitions to state β. The fault Y, with severity γ, will only occur when both the state and temporal conditions are simultaneously satisfied. Any deviation in the variables will result in the conditions not being met, causing the fault symptoms to disappear. Due to the dynamic evolution of faults and the inherent uncertainty in fault propagation processes, these combination conditions are not always fulfilled, leading to the intermittency of fault symptoms.

An intermittent fault in a filter circuit, caused by an intermittent open-circuit coupling of two components, serves as an example to illustrate the types of faults discussed in this paper. The schematic diagram of the four opamp biquad high-pass filter circuit is shown in Fig. 2 [27].

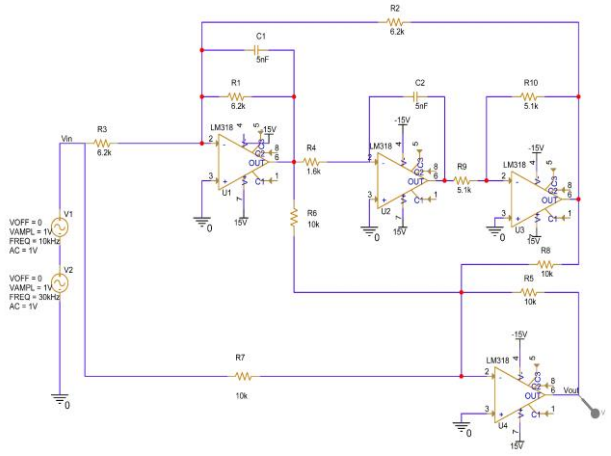

Fig. 2. The four opamp biquad high-pass filter simulation circuit.

The corresponding output voltage signal at the V_{out} point in Fig. 2 is shown in Fig. 3.

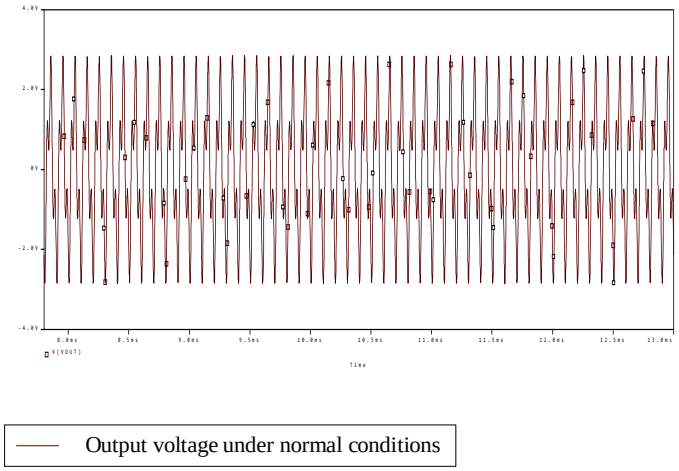

Fig. 3. The normal voltage signal of V_{out}.

To inject intermittent open-circuit faults into the circuit, a combination of a voltage-controlled switch and a voltage pulse signal source is used, as illustrated by the red rectangular box in Fig. 4.

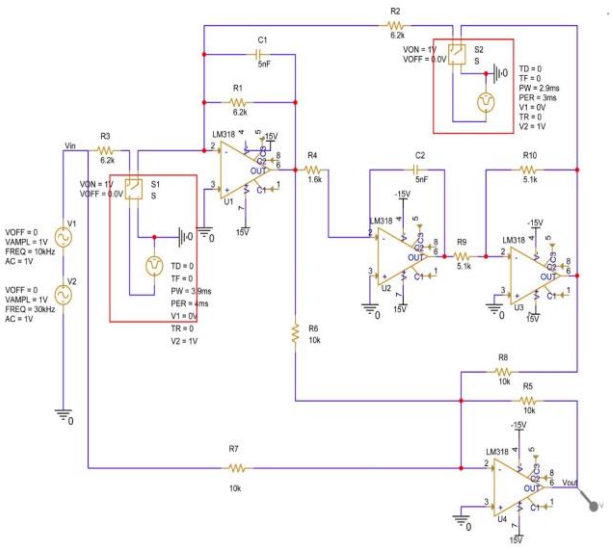

Fig. 4. Simulation circuit under intermittent fault.

The timing of fault injection can be controlled by adjusting the parameters. The output voltage signal, V_{out}, is recorded over the same duration under various fault injection scenarios, as shown in Fig. 5. Fig. 5(a), 5(b), and 5(c) represent the voltage data collected at the output point for three scenarios: when only R3 injects a fault, when only R2 injects a fault, and when both R3 and R2 inject faults, respectively. Fig. 5(d) compares the waveforms of Fig. 3 and Fig. 5(c), highlighting the noticeable differences between them. As shown in Fig. 5, it is evident that when only one resistor is open, the circuit's output voltage deviates slightly from the normal value within a narrow range. On the other hand, when both resistors are open, the circuit's output voltage deviates significantly from the normal range, resulting in a pronounced intermittent fault.

The interpretation of intermittent faults in this paper aligns with the IEEE standard definition of such faults.

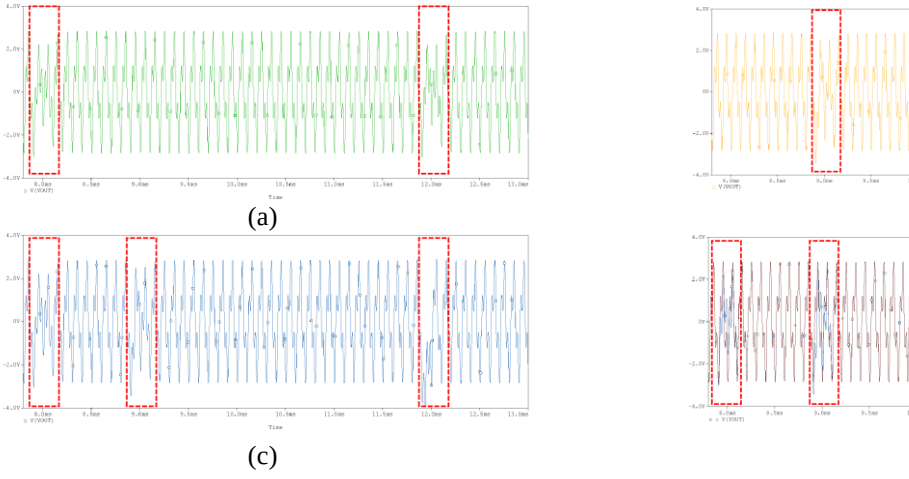

Fig. 5. The abnormal voltage signal of V_{out}.

B. The DUCG Model

The DUCG was originally proposed by Zhang [20] to intuitively represent uncertain causalities among variables and to perform probabilistic reasoning. In this section, the basic theories of DUCG are briefly described.

As shown in Fig. 6, DUCG consists of a set of variables or events classified into B-type, X-type, G-type, and D-type categories [21]. Different types of variables are represented in the graphical model by nodes of various shapes. The explanations of the symbols used in the graphical model are provided in Table 2.

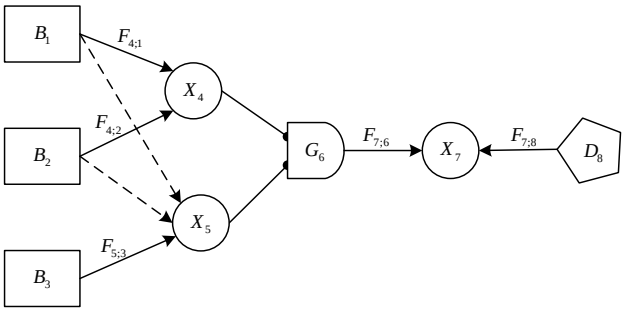

Fig. 6. The DUCG model.

Table 2. The explanations of symbols

Symbols	Explanations
B_i	root variable and drawn as rectangle, which can only be a cause or parent variable.
X_i	consequence variable and drawn as circle. It can also be a cause or parent variable.
G_i	logic gate variable and drawn as the shape of an AND-gate, which represents the combinational logical relationships between its inputs and outputs.
D_i	default variable and drawn as pentagon, which is the unknown or inexplicit cause of X_n.
V_i	Suppose V_i, $V \in \{B, X, G, D\}$, are the parent variables of X_n.
$V_{i,j}$	The subscript i before "," is used to distinguish among different variables. The subscript j after "," denotes the state of V_i. $j = 0$ indicates the normal state of the variable, and $j \neq 0$ indicates the abnormal state.
$\rightarrow$	weighted functional variable denoted as $F_{n;i}$. It is used to express the direct causal relationship between the parent variable V_i and the child variable X_n. When the states of the parent and child variables are determined, it is written as $F_{n,k;i,j}$. The subscript before ";" is for the child variable and the subscript after ";" is for the parent variable.

Symbols	Explanations
⇢	A conditional connection variable, which means that if the condition $Z_{n;i}$ is met, the variable becomes a weighted functional variable. Otherwise, it is deleted.

The logic gate specification (LGS) table is used to explain combinational logic relationships (e.g., G_6 in Fig. 6, with the state specifications listed in Table 3). Different combinations of state among parent variables correspond to different values of the logic gate, which, in turn, have varying effects on the consequence variables.

Table 3. Logic gate specification.

Logic gate	State	State expression
G_6	1	$(X_{4,2}+X_{4,3})X_{5,2}$
	2	$X_{4,3}X_{5,3}$
	3	Remnant state

$X_{n,k}$ denotes the event that X_n is in state k. As shown in Fig. 7, $X_{n,k}$ can be influenced by multiple variables, such as $V_{1,j}$, $V_{2,j}$, and $V_{i,j}$. The event that $X_{n,k}$ is caused solely by $V_{i,j}$ is denoted as $X_{n,k;i,j}$. The causal relationship between the parent variable $V_{i,j}$ and the child variable $X_{n,k}$ can be represented by a functional variable $F_{n,k;i,j}=(r_{n;i}/r_n)A_{n,k;i,j}$ [28], which consists of two parts: the weighting factor $(r_{n;i}/r_n)$ and $A_{n,k;i,j}$. $r_{n;i}$ represents the causality strength between V_i and X_n, and $r_n=\sum_i r_{n;i}$. The term $(r_{n;i}/r_n)$ is used to standardize the influence that the parent variables exert on the child variables. $A_{n,k;i,j}$ is defined as the random event that $V_{i,j}$ does indeed cause $X_{n,k}$ given that $V_{i,j}$ is true, regardless of the other parent variables. In other words, $A_{n,k;i,j}$ quantifies the causal mechanism by which $V_{i,j}$ independently causes $X_{n,k}$. The purpose of this equation is to determine the probability of each parent event's role in triggering the child event.

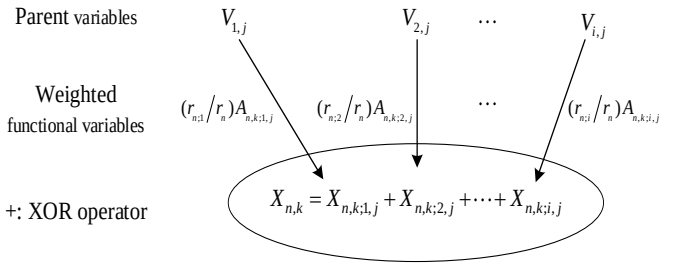

Fig. 7. Illustration for the DUCG model.

The DUCG model uses the chaining inference rule to expand detected variables along the logical causal chain to identify root cause variables. The core of the inference rule is the ``weighted logical expansion", which can be described as:

$$X_{n,k}=\sum_i F_{n,k;i}V_i=\sum_i(r_{n;i}/r_n)\sum_j A_{n,k;i,j}V_{i,j} \quad (1)$$

In DUCG, variables are typically expressed in capital letters, with the corresponding lowercase letters representing their probabilities. The diagnostic inference algorithm of DUCG analyzes the causal logical relationships among variables to determine whether an alternative fault hypothesis can fully explain the existing abnormal conditions. A possible cause hypothesis based on the observed evidence $E=\prod_n X_{n,k}$ can be represented as $H_{k,j}$. The probability of $H_{k,j}$ can be calculated as follows:

$$h^s_{k,j}=Pr\{H_{k,j}|E\}=\frac{Pr\{H_{k,j}E\}}{Pr\{E\}} \quad (2)$$

C. Timed Failure Propagation Graphs

The TFPGs [25] capture the effect of temporal constraints and switching dynamics on the propagation of failures using the causality graph shown in Fig. 8. In this graph, the rectangular nodes (FM_i) denote failure modes, which are fault causes. The circle and square nodes (D_i) represent OR-type and AND-type discrepancies, respectively. Discrepancy nodes typically represent the effects of failure modes. The state of each node in the TFPG model is either ON or OFF. An ON state indicates that the node is activated, which is represented by a shaded node in the model, while an OFF state indicates that the effects of any faults have not propagated to the node. The edge between two nodes in the graph captures the effect of failure propagation over time within the dynamic system and is parameterized with a time interval $[e.tmin, e.tmax]$. Specifically, given that a propagation edge is active, it will take at most $e.tmax$ and at least $e.tmin$ for the fault to propagation from the source node to the destination node. The capital letters on the edges (A/B) represent a set of system modes. These edges may be activated only if the system is in corresponding mode.

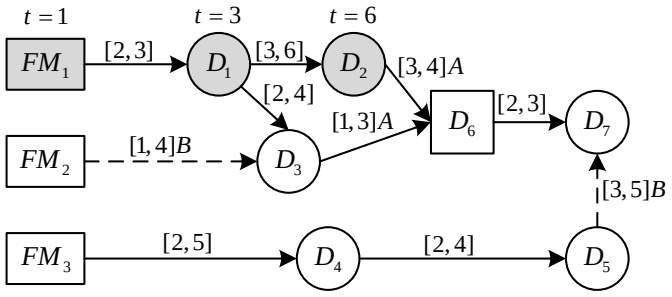

Fig. 8. The TFPG model.

D. Problem Formulation

The main problem addressed in this paper is the diagnosis of intermittent faults caused by the coupling of multivariate anomalous states during the fault propagation process.

To address this issue, a new fault propagation model, called TC-DUCG, is proposed to flexibly model the complex temporal and logical dependencies inherent in fault propagation. Additionally a diagnostic inference method is introduced to explore potential causes of intermittent faults based on observational evidence.

The model not only considers the probability of fault propagation among variables, but also integrates temporal constraints. Moreover, the model introduces a type of logical temporal gate node to represent complex logical and temporal coupling relationships between node variables. During the inference process, observation interval division criteria are applied to segment the evidence. This allows for time range and logical matching analysis of evidence within the same time slice, helping to eliminate false alarms and thereby improving the accuracy of the diagnosis.

3. The TC-DUCG model

As mentioned in Section 1, a fault propagation diagnostic model consists of three main parts: the model framework, model parameters, and inference methods. The model framework and model parameters together constitute the fault propagation model. In this paper, a model called the Temporal Constrained Dynamic Uncertain Causality Graph (TC-DUCG) is proposed to capture the temporal and logical dependencies in the fault propagation process. The overall scheme of the proposed TC-DUCG and the diagnostic reasoning based on this model are illustrated in Fig. 9.

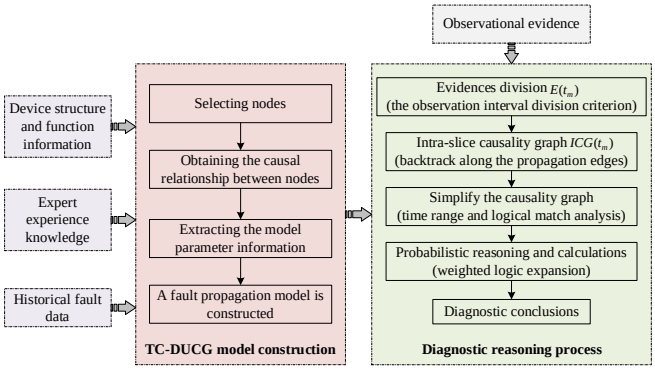

Fig. 9. The overall scheme of TC-DUCG model construction and diagnostic reasoning process.

A. TC-DUCG Modeling

Fig. 10 presents a graphical representation of the TC-DUCG model. A TC-DUCG is represented as a tuple $(\boldsymbol{V}, \boldsymbol{E}, \boldsymbol{W})$. The symbols used in this model are explained in Table 4.

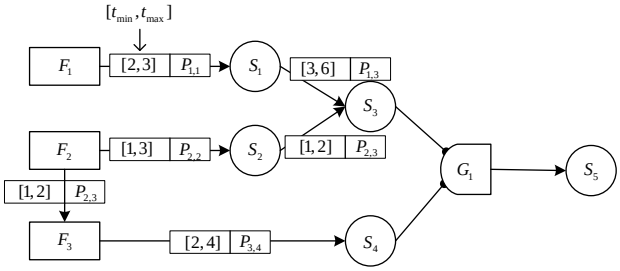

Fig. 10. A typical TC-DUCG model.

Table 4. The explanations of symbols

Symbols	Explanations
$\boldsymbol{V}$	A set of model nodes. $\boldsymbol{V} = \{\boldsymbol{F}, \boldsymbol{S}, \boldsymbol{G}\}$.
$\boldsymbol{E}$	Edge sets, which represent dependencies between nodes.
$\boldsymbol{W}$	A set of model parameters.
$\boldsymbol{F}$	A set of failure modes nodes.
F_i	A failure modes node, where $F_i \in \boldsymbol{F}$.
F_i^k	The node state of F_i.
$\boldsymbol{S}$	A set of discrepancy nodes representing the effects of failure modes. Nodes in the set represent system entities with monitoring signals or observable events.
S_i	A discrepancy node, where $S_i \in \boldsymbol{S}$.
S_i^k	The node state of S_i.
$\boldsymbol{G}$	A set of logical temporal gate nodes, which express complex logical and temporal coupling relationships between node variables.
$\boldsymbol{P}(F_i)$	The prior probability matrix of failure mode node F_i.
m_i	The state number of the node F_i.
$P(F_i^m)$	The probability that the failure node F_i is in state m.
w_{ij}	Causal correlation parameter that indicates the intensity of the causal relationship between V_i and S_j.
$\boldsymbol{P}_{ij}$	The conditional probability matrix, which represents the independent effect of a parent variable V_i on a child variable S_j, without considering the influence of other parent variables.
E	Observational evidence.
t_{V_i}	The time at which the node V_i is activated.
$t_{V_i^k}$	The time when the state of the variable changes to V_i^k.
$[t_{min}, t_{max}]$	The fault propagation time interval, where t_{min} and t_{max} denote the minimum and maximum time for the fault impact to propagate from the parent node to the child node, respectively.

Symbols	Explanations
T	An observation interval that can be divided into a set of time slices $T=\{t_1,t_2,\cdots\}$.
$E(t_m)$	The evidence received within the time slice t_m.
$ICG(t_m)$	An intra-slice causality graph within the time slice t_m.
$S_H(t_m)$	A possible fault hypothesis space within the time slice t_m.

The TC-DUCG model consists of two types of events: failure modes and the effects of failure modes. A failure mode node $F_i \in \boldsymbol{F}$ represents a defect or abnormal condition that may be the root cause of a system failure, such as resistor parameter drift. The node state F_i^k indicates different manifestations of the failure mode, such as parameter drift exceeding the upper threshold of 10% or falling below the lower threshold of 20%. The discrepancy node $S_i \in \boldsymbol{S}$ represents off-nominal conditions that result from failure modes. A discrepancy can be monitored and is typically associated with alarms. The state S_i^k represents the degree to which the failure mode has caused deviation from the nominal value. The sets of nodes $\boldsymbol{F}$ and $\boldsymbol{S}$ are selected for model construction based on the device's structure and function information, as well as expert experience. The various state attributes of each node are defined according to the actual meanings represented by the nodes.

The edges in the model are structured to express the dependency relationship among nodes. Two nodes with a direct causal relationship are connected by a directed edge, with the cause node pointing to the consequence node. In addition, the model introduces a type of logical temporal gate node $\boldsymbol{G}$ (referred to as gate node) to express complex logical and temporal coupling relationships between node variables during the fault propagation process. Specifically, the cause node is connected to the gate node by a directed arc with a black dot at the tail end, and the gate node is connected to the consequence node by a directed edge.

The logical temporal gate involves a mechanism that controls the flow of fault propagation based on the temporal order and state logic of variables, which can be defined as a function or rule. It selectively allows or blocks the propagation of faults depending on the specific temporal and state combination conditions. The combination conditions can be explained using a gate specification table that consists of four parts: gate variables, gate states, state expressions, and temporal expressions. The state expressions can flexibly represent the combinational logic relationships between different states of variables. The temporal expressions can effectively express the constraint relationships between activation times of parent variables. Table 5 presents an example (i.e., the state and temporal specification of G_1 in Fig. 10). The logical temporal gate G_1 has four mutually exclusive states, corresponding to different state and temporal combinations of variable S_3 and variable S_4. For instance, the state of variable G_1 is G_1^1 if and only if S_4^1 occurs first and lasts more than 5 time units before either S_3^1 or S_3^2 is activated. If S_3^3 is activated first, followed by the activation of S_4^2, then the state of variable G_1 is G_1^3.

Table 5. The improved gate specification table.

Logical temporal gate	State	State expression	Temporal expression
G_1	0	Remnant state	Else
	1	$(S_3^1+S_3^2)S_4^1$	$t_{S_3}-t_{S_4}>5$
	2	$S_3^2S_4^2$	$t_{S_3}-t_{S_4}>1$
	3	$S_3^3S_4^2$	$t_{S_4}>t_{S_3}$

The three types of nodes in the model can collectively represent as node V. The causal relationships between nodes and associated parameters are specified directly based on expert experience or learned from historical fault data and physical simulation of failures.

The model parameters include the prior probability of fault mode nodes, the causal relationship intensity, the conditional probability matrix between model nodes, and the fault propagation time interval. The prior probability $\boldsymbol{P}(F_i)$ of failure mode node is an $m_i * 1$ dimensional matrix, where m_i is the state number of the node F_i. The element $P(F_i^m)$ in the $m+1$ row of the matrix represents the probability of the failure node being in state m. In certain cases, the domain expert may be uncertain about the existence of a causal link between V_i and S_j. To represent the uncertainty of causal relationships, the model introduces causal correlation parameters w_{ij}, which indicates the causal relationship intensity between V_i (V can be an $F/S/G$ type node) and S_j. $w_{ij}=1$ indicates that the causal relationship between two nodes is determined. $w_{ij}=0$ represents a definite absence of a causal relationship between two nodes. For situations where the causal relationship is uncertain, $0<w_{ij}<1$. $(w_{ij}/\sum_i w_{ij})$ is employed to standardize the influence that parent variables exert on child variables. The conditional

probability matrix $\boldsymbol{P}_{ij}$ represents the independent effect of a parent variable V_i on a child variable S_j, without considering the influence of other parent variables. The $m+1$ row and $n+1$ column element of the matrix $\boldsymbol{P}_{ij}$ represents the probability that V_i^m causes S_j^n, given that V_i^m is true. The matrix dimension is $m_i * m_j$. The element $P(V_i^m)$ in the $m+1$ row of the matrix $\boldsymbol{P}(V_i)$ represents the probability of the node being in state m. The formula for calculating the probability matrix of a discrepancy node is as follows:

$$\mathbf{P}(S_j) = \sum_i (w_{ij} / \sum_i w_{ij})\, \mathbf{P}_{ij}^{\top} \mathbf{P}(V_i) \tag{3}$$

The condition probability of a fault hypothesis F_i^m on the condition of the state of evidence E can be expressed as:

$$P(F_i^m|E) = \frac{P(F_i^m)P(E|F_i^m)}{P(E)} \tag{4}$$

The time point t_{V_i} indicates the time when node V_i is activated (a failure mode occurs or the impact of a failure propagates to a discrepancy node). $t_{V_i^k}$ is the time when the state of the variable changes to V_i^k. The fault propagation time interval is $[t_{min}, t_{max}]$, where t_{min} and t_{max} denote the minimum and maximum time for the fault impact to propagate from the parent node to the child node, respectively. As indicated in the literature [25], the time interval $[t_{min}, t_{max}]$ can be determined either analytically or by simulating an accurate physical model.

It's important to recognize that not all relationships can be captured perfectly. Nevertheless, the effectiveness of the TC-DUCG model can be significantly enhanced by combining expert knowledge, historical data, continuous updates, and a robust methodology for dealing with uncertainty and incomplete information. The DUCG model can be incomplete due to the chaining inference of DUCG is self-relied [20]. The TC-DUCG model introduces temporal constraints based on the DUCG model, which can also be incomplete.

B. Fault Diagnosis Reasoning Method

During the occurrence, propagation, and evolution of faults, the states of system variables change dynamically. The causal relationships among variables are complex and uncertain, as shown in Fig. 11. In the figure, $S_i(\alpha)$ and $S_j(\beta)$ represent the state change process of variable S_i and variable S_j within a certain observation interval T, respectively. $\alpha = 1,2,\ldots,a$, $\beta = 1,2,\ldots,b$ indicate the order in which the variables appear. $t_{S_i(\alpha)}$ represents the time when the corresponding state of the variable occurs. The dashed lines with arrows indicate the uncertain causal relationships between variable S_i and S_j in their corresponding states. In order to express the dynamic uncertain causal relationships between variables more intuitively and flexibly, the observation interval T is divided into a set of time slices $T = \{t_1, t_2, \cdots\}$. The criteria for dividing the observation interval are summarized as follows.

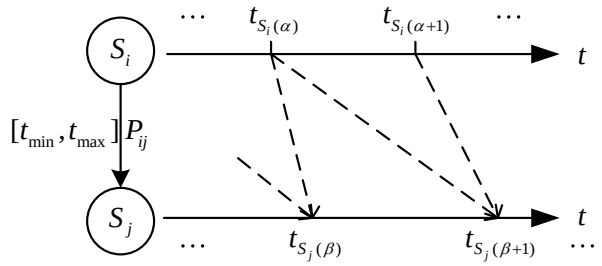

Fig. 11. The state change process of observed variables.

- All variables within the time slice t_1 are in the first state change phase. If any variable changes state for the second time, it switches to time slice t_2. According to this criterion, the observed evidence is preliminarily divided.
- It takes time for a fault to propagate from the causal variable to the consequence variable. The consequence variable continues to propagate backward in its state until the effect of a change in the state of the causal variable in the subsequent time slices propagates to that variable. Nodes that are affected by the current state of the consequence variable are represented in the current time slice.
- The consequence variables that are in an abnormal state in the previous time slice and have not changed in the current time slice will be represented in both time slices.

The evidence received within the time slice t_m is $E(t_m)$. The purpose of the diagnostic reasoning process is to determine the most likely fault location based on the alarm records. The dynamic causality graph modeling and reasoning process is listed as follows.

1) An intra-slice causality graph $ICG(t_m)$ can be obtained by backtracking, along propagation edges, starting from the nodes within $E(t_m)$ that indicate abnormal states. In this step, irrelevant variables and causalities in the original

TC-DUCG graph are removed, and the possible fault hypothesis space $S_H(t_m)$ is determined.

2) Perform rigorous time range and logical match analysis on the variables in $ICG(t_m)$ to eliminate incorrect and meaningless causal relationships in the graph. This step helps eliminate invalid fault hypotheses and improve the accuracy of the diagnostic results. The specific analysis process is detailed in Section C.
3) The probabilities of the remaining fault hypothesis are calculated according to equations (3) and (4), and the most likely root cause of the fault within the time slice is obtained.
4) Comprehensive analysis of the diagnostic conclusions of different time slices in the observation interval can derive the possible root causes and evolution process of faults.

C. Time Range and Logical Matching Analysis

According to the observation interval division criterion, it can be seen that the states of the variables in $ICG(t_m)$ change only once. This simplifies the matching analysis process.

In this paper, the causal relationships between observed variables are divided into two types: one is direct causality and the other is combinational logical causality. The time range and logical match analysis steps in both cases are listed separately.

For two nodes S_i and S_j with a direct causality connected by a directed edge, the matching analysis process is listed as Algorithm 1.

Algorithm 1 Time Range and Logical Matching Analysis of Direct Causal Relationships.

Inputs: the node states $S_i^m(0 \le m \le m_i)$, $S_j^n(0 \le n \le m_j)$; the activation times for the states $t_{S_i^m}$, $t_{S_j^n}$; the time interval for the propagation of faults between the two nodes $[t_{min}, t_{max}]$; and the conditional probability matrix $\boldsymbol{P}_{ij}$.

Outputs: Whether to remove the propagation edge between nodes S_i and S_j. (0: preserve; 1: remove)

1. Read the value p_1 of the element in the mth row and nth column of the matrix $\boldsymbol{P}_{ij}$.
2. If $p_1 \neq 0$ then
3. If $t_{S_j^n} - t_{S_i^m} \in [t_{min}, t_{max}]$ then
4. Return 0
5. Else
6. Return 1
7. End

If the algorithm returns 0, the observed evidence matches the model constraints, then preserve the propagation edge. If it returns 1, the time range or logical relationship does not match. It is considered that S_j^n is not caused by S_i^m. Remove the propagation edge between S_i^m and S_j^n.

For parent nodes S_i, S_j and child node S_k with combinational logical causalities connected by a gate variable G_i, the matching analysis process is listed as Algorithm 2.

Algorithm 2 Time Range and Logical Matching Analysis of Combinational Logical Causalities.

Inputs: the node states $S_i^m(0 \le m \le m_i)$, $S_j^n(0 \le n \le m_j)$, $S_k^p(0 \le p \le m_k)$; the activation times for the states $t_{S_i^m}$, $t_{S_j^n}$, $t_{S_k^p}$; the time interval for the propagation of faults between the parent nodes and child node $[t_{min}, t_{max}]$; the conditional probability matrix $\boldsymbol{P}_{ik}$; the gate specification table of G_i.

Outputs: Whether to remove the edges between these nodes. (0: preserve; 1: remove)

1. Based on the information of S_i^m, S_j^n, $t_{S_i^m}$, and $t_{S_j^n}$, check the gate specification table to determine the state of gate variable G_i as G_i^q.
2. Read the value p_2 of the element in the qth row and pth column of the matrix $\boldsymbol{P}_{ik}$.
3. If $p_2 \neq 0$ then
4. Calculate $t_{G_i^q} \in [t_{S_k} - t_{max}, t_{S_k} - t_{min}]$.
5. Check $t_{G_i^q}$, $t_{S_i^m}$, $t_{S_j^n}$, and the temporal expressions of the gate specification table.
6. If the temporal information satisfies the model constraints then
7. Return 0
8. Else
9. Return 1
10. End

If the algorithm returns 0, preserve the edges between these nodes. If it returns 1, remove the edges between these nodes.

4. CASE STUDY AND DISCUSSION

In this section, a real case of intermittent fault diagnosis in a millimeter-wave radar is investigated. A detailed description of the entire application process of the TC-DUCG model is provided, which demonstrates the effectiveness of the proposed TC-DUCG model in the modeling and reasoning of intermittent faults caused by temporal and state coupling.

A. Device Introduction

In recent years, millimeter-wave radar has found extensive applications in intelligent security, unmanned technology, and drones. The case object of this paper is a single transmitter channel, dual receiver channel FMCW millimeter-wave radar [29]. The radar system utilizes an external DC power supply ranging from 5V to 12V, which is initially regulated to 4V DC

using the 4V DC regulator module. Subsequently, the 4V DC is further converted to 3.3V DC and 1.8V/3.3V DC. The converted 3.3V DC is then directed to the crystal oscillator circuit, responsible for generating the fundamental frequency REF. The fundamental frequency REF is subsequently fed into the frequency synthesizer, which generates the charge pump voltage COV. The COV is input to the voltage-controlled oscillator of the RF transceiver, generating the RF signal within the RF transceiver. After power amplification in the RF transceiver, the RF signal is transmitted from the transmitting antenna. Simultaneously, the RF signal received by the receiving antenna is mixed with the transmitted RF signal to obtain the intermediate frequency (IF) signal. It is divided by a frequency divider and then input to the frequency synthesizer. The IF signal is split into two channels and fed into the amplifier circuit. The signal is then sent to the digital signal processor for further processing. The processed signal undergoes back-end processing and is then connected to host computer software, which displays the millimeter-wave radar results. The functional and structural block diagrams of the millimeter-wave radar system are depicted in Fig. 12, with a more detailed functional structure block diagram shown in Fig. 13.

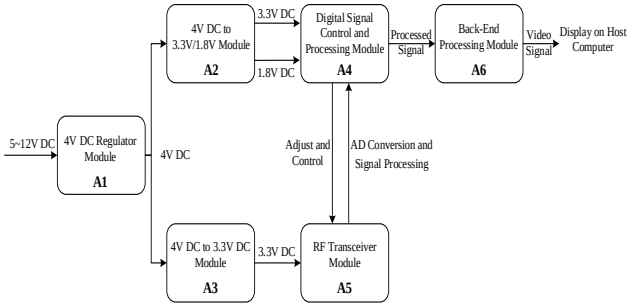

Fig. 12. Structure-function simplified block diagram of a millimeter-wave radar.

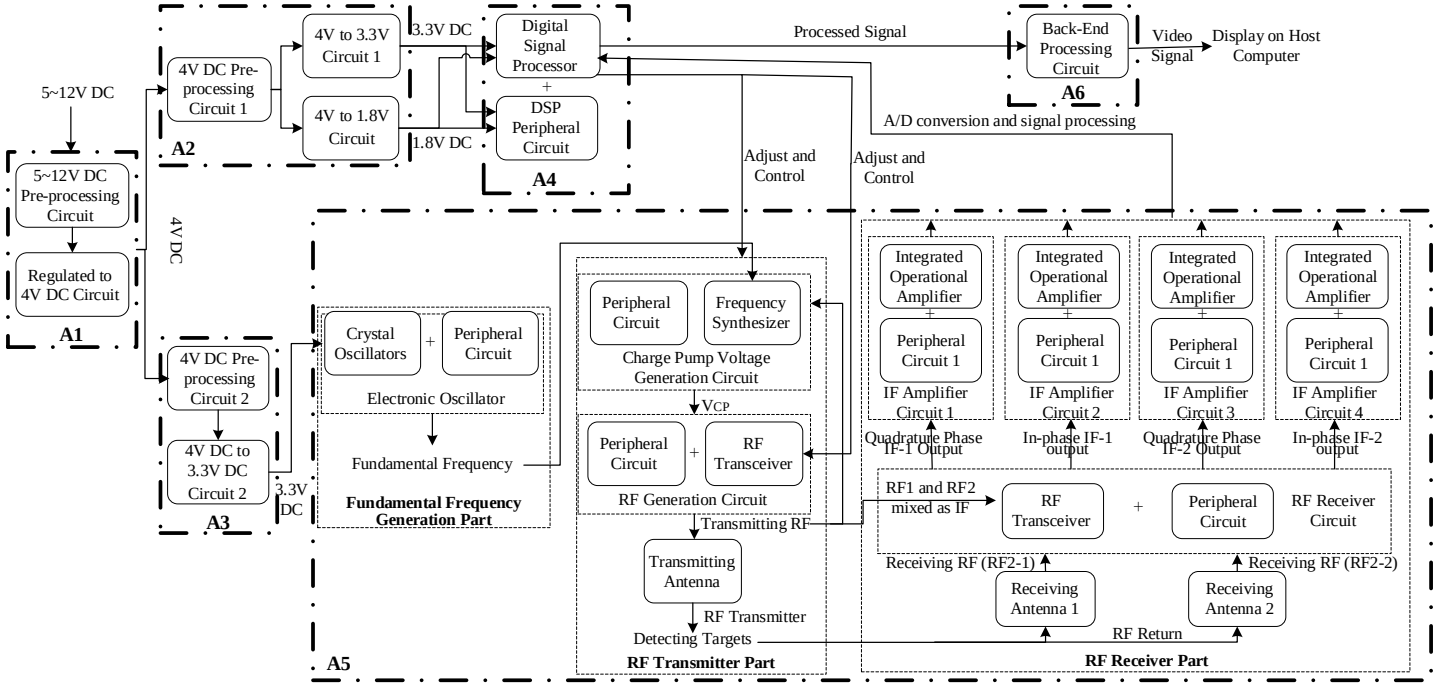

Fig. 13. Structure-function detailed block diagram of a millimeter-wave radar.

B. Fault Description

Multiple failure modes, propagated through a series of fault propagation paths, can lead to intermittent fault in the functionality of the radar. For example, a soldering defect on pin 3 of the chip in the crystal oscillator can cause intermittent short circuiting of the AC signal generated by the oscillator. This results in intermittent oscillation failure in the oscillator circuit, leading to intermittent failure in the generation of the fundamental frequency in the frequency generation circuit. Consequently, the frequency synthesizer experiences intermittent loss of the fundamental frequency input, resulting in intermittent failure in RF signal generation and transmission. The intermittent failure in RF transmission leads to intermittent absence of the intermediate frequency (IF) signal output. The IF amplification circuit then intermittently fails to produce a valid output signal. Furthermore, the intermittent failure propagates to the digital signal control and processing module, causing intermittent absence of valid signal outputs. Ultimately, this

sequence of failures results in intermittent fault of functionality in radar operations. In addition, intermittent failures in the back-end processing module and intermittent non-operation of the digital signal control and processing module can also lead to intermittent fault of radar.

C. Node Selection and Model Construction

The millimeter-wave radar consists of numerous components and modules, and the fault propagation paths are complex. To simplify the analysis, certain components are abstracted as nodes in the TC-DUCG model, as shown in the Fig. 14. The model parameters are generated randomly, and in practice the parameters can be obtained by learning from historical data or specified directly by domain experts based on their empirical knowledge. The fault propagation temporal constraints among variables are marked on the propagation edges.

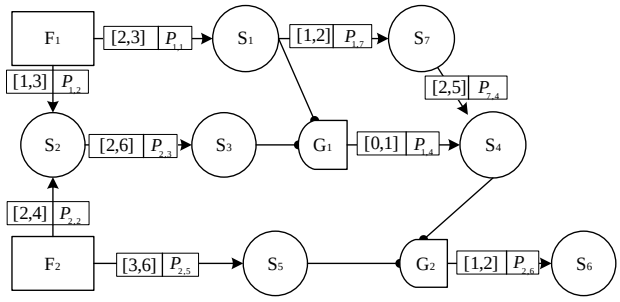

Fig. 14. An illustrative example of TC-DUCG.

The occurrence probabilities of each failure mode nodes are:

$$\boldsymbol{P}(F_1) = \begin{pmatrix} \overline{} \\ 0.02 \\ 0.001 \end{pmatrix} \quad \boldsymbol{P}(F_2) = \begin{pmatrix} \overline{} \\ 0.01 \\ 0.005 \end{pmatrix}$$

The conditional probability matrix $\boldsymbol{P}_{ij}$ of the model are listed as follows. The unlisted parameter represented by the symbol $-$ indicates that the parameter is not available or about which we do not care.

$$\boldsymbol{P}_{11} = \begin{pmatrix} \overline{} & \overline{} & \overline{} \\ - & 0.3 & 0 \\ - & 0.5 & 0.1 \end{pmatrix} \boldsymbol{P}_{12} = \begin{pmatrix} \overline{} & \overline{} & \overline{} \\ - & 0.4 & 0.1 \\ - & 0.7 & 0.2 \end{pmatrix}$$

$$\boldsymbol{P}_{22} = \begin{pmatrix} \overline{} & \overline{} & \overline{} \\ - & 0 & 0.2 \\ - & 0 & 0.5 \end{pmatrix}$$

$$\boldsymbol{P}_{23} = \begin{pmatrix} \overline{} & \overline{} & \overline{} \\ - & 0 & 0.4 \\ - & 0.6 & 0 \end{pmatrix} \boldsymbol{P}_{14} = \begin{pmatrix} \overline{} & \overline{} & \overline{} \\ - & 0.9 & 0 \\ - & 0 & 0.8 \end{pmatrix}$$

$$\boldsymbol{P}_{74} = \begin{pmatrix} \overline{} & \overline{} & \overline{} \\ - & 0 & 0.6 \\ - & 0 & 0.4 \end{pmatrix}$$

$$\boldsymbol{P}_{25} = \begin{pmatrix} \overline{} & \overline{} & \overline{} \\ - & 0 & 0.6 \\ - & 0.8 & 0 \end{pmatrix} \boldsymbol{P}_{26} = \begin{pmatrix} \overline{} & \overline{} & \overline{} \\ - & 0.5 & 0 \\ - & 0.4 & 0 \end{pmatrix} \boldsymbol{P}_{17}$$
$$= \begin{pmatrix} \overline{} & \overline{} & \overline{} \\ - & 0 & 0 \\ - & 0.3 & 0.2 \end{pmatrix}$$

The logic temporal gate specification table of G_1 and G_2 in Fig. 14 are shown in Table 6.

Table 6. Logic gate specification,

Logical temporal gate	State	State expression	Temporal expression
G_1	0	Remnant state	Else
	1	$(S_1^1 + S_1^2)S_3^1$	$t_{S_1} - t_{S_3} > 2$
	2	$S_1^1 S_3^2$	$t_{S_3} - t_{S_1} > 1$
G_2	0	Remnant state	Else
	1	$S_4^1 S_5^1$	$t_{S_4} > t_{S_5}$
	2	S_4^2	$t_{S_4} < t_{S_5}$

D. Evidence

Observational evidence can be classified into abnormal evidence and normal evidence. Assuming the following alarm records were observed within a certain observation interval: $S_2^1(t_{S_2^1} = 2), S_1^1(t_{S_1^1} = 3), S_3^2(t_{S_3^2} = 5), S_4^2(t_{S_4^2} = 6), S_6^1(t_{S_6^1} = 8), S_1^2(t_{S_1^2} = 9), S_4^0(t_{S_4^0} = 9), S_6^0(t_{S_6^0} = 10), S_7^1(t_{S_7^1} = 11)$.

According to the criteria for dividing the observation interval, the observation interval is divided into a set of time slices $T = \{t_1, t_2\}$. The observed variables are represented in the corresponding time slices.

The observed evidence within time slice t_1 includes:

- Abnormal Evidence: $S_2^1(t_{S_2^1} = 2)$, $S_1^1(t_{S_1^1} = 3)$, $S_3^2(t_{S_3^2} = 5), S_4^2(t_{S_4^2} = 6), S_6^1(t_{S_6^1} = 8)$.
- Normal Evidence: S_5^0, S_7^0.

The observed evidence within time slice t_2 includes:

- Abnormal Evidence: $S_1^2(t_{S_1^2} = 9), S_7^1(t_{S_7^1} = 11), S_2^1, S_3^2$.
- Normal Evidence: $S_4^0(t_{S_4^0} = 9), S_5^0, S_6^0(t_{S_6^0} = 10)$.

E. Diagnostic Reasoning Process

The detailed diagnostic reasoning process for this example is presented here.

1) Obtaining the Intra-slice Causality Graph $\boldsymbol{ICG}(\boldsymbol{t_m})$

Performing backtrack reasoning based on the observed evidence, the intra-slice causal graph $\boldsymbol{ICG}(\boldsymbol{t_m})$ is obtained as shown in Fig. 15. This step starts from the nodes representing abnormal states and traces back along the propagation edges. During the backtracking process, irrelevant variables and causal relationships are eliminated from the original TC-DUCG graph.

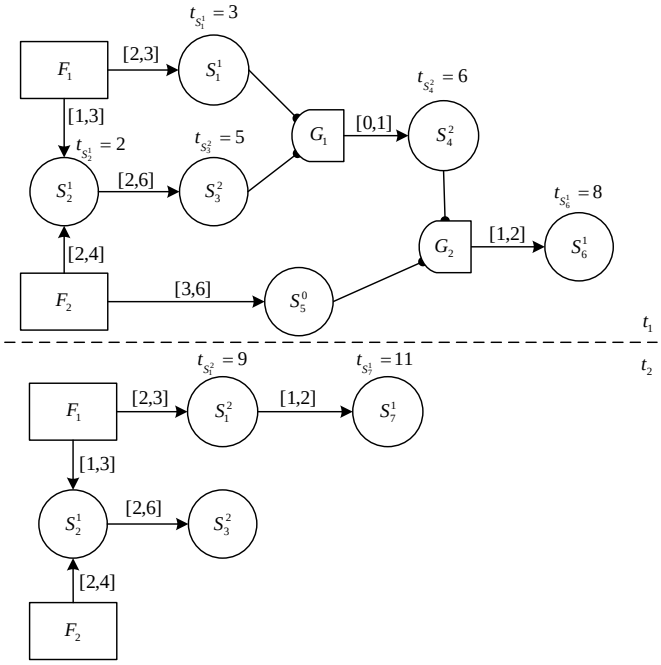

Fig. 15. The intra-slice causality graph.

2) Time Range and Logical Matching Analysis

This step involves a rigorous analysis of time range and logical matching to validate whether the observed evidence meets the model constraints and to eliminate incorrect and meaningless causal relationships in the graph $\boldsymbol{ICG(t_m)}$.

The matching analysis results within time slice t_1 indicate that the possible fault hypothesis space is $S_H(t_1) = \{F_1^1, F_1^2\}$, with a fault triggering time of $t_{F_1} \in [0,1]$. The matching analysis results within time slice t_2 indicate that the possible fault hypothesis space is $S_H(t_2) = \{F_1^2\}$, with a fault triggering time of $t_{F_1} \in [6,7]$.

3) Probabilistic Reasoning and Calculations

After completing the aforementioned steps of time range and logical matching analysis, a simplified intra-slice causality graph can be obtained, as shown in Fig. 16. The temporal relationships between variables in the simplified graph satisfy the model constraints. This step calculates the probabilities of candidate fault hypothesis in the fault hypothesis space, independent of temporal information. The propagation time constraints between nodes and the timing of variable state changes are not shown in the simplified graph. The process of probabilistic reasoning and calculation is as follows.

For simplicity, all weight factors w_{ij} are set to 1. The evidence in time slice t_1 is:

$$E(t_1) = S_1^1 S_2^1 S_3^2 S_4^2 S_6^1 \tag{5}$$

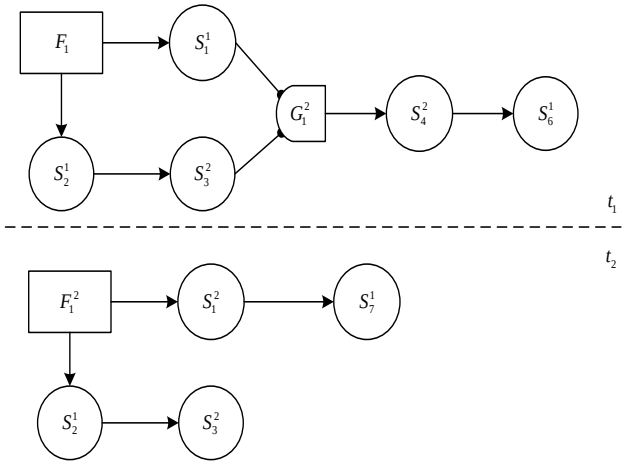

Fig. 16. The simplified intra-slice causality graph.

According to equations (3) and (4), the probability of the fault hypothesis F_1^1 within time slice t_1 is calculated as:

$$P\{F_1^1|E(t_1)\} = \frac{P(F_1^1)P(E(t_1)|F_1^1)}{P(E(t_1))} = 0.87273 \tag{6}$$

The probability of the fault hypothesis F_1^2 within time slice t_1 is calculated as:

$$P\{F_1^2|E(t_1)\} = \frac{P(F_1^2)P(E(t_1)|F_1^2)}{P(E(t_1))} = 0.12727 \tag{7}$$

It is easy to determine the most likely fault to occur as F_1^1 by comparing the posterior probabilities of the two fault hypotheses. According to Section 2), the fault hypothesis space within time slice t_2 is $S_H(t_2) = \{F_1^2\}$. As there is only one hypothesis event in $S_H(t_2)$, it is evident that the most likely fault to occur in time slice t_2 is F_1^2.

4) Diagnostic Conclusion

Based on the aforementioned diagnostic reasoning process, it can be concluded that the failure mode node F_1 undergoes a state change to F_1^1 in the time interval [0,1] and a state change to F_1^2 in the time interval [6,7].

F. Experimental Validation

On a PC machine with an Intel(R) Core (TM) i7-9750H CPU (2.60GHz) and 16.0GB of memory, the TC-DUCG model construction and fault diagnosis inference process was implemented using PyCharm 2022.1.3. The parameters and evidence from the case in Section 4 C and D have been entered into the inference program. The experimental results are shown in Fig. 17 - 19. Fig. 17 presents the simplified intra-slice causality graph.

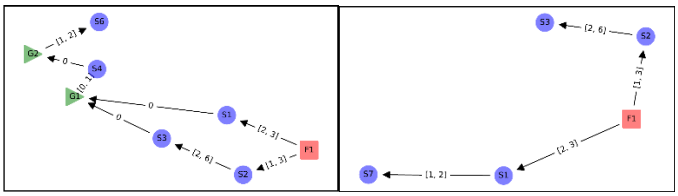

Fig. 17. (a) t1 time slice; (b) t2 time slice.

The results of the fault diagnosis inference on each time slice are shown in Fig. 18.

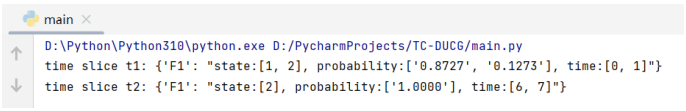

Fig. 18. The results of the fault diagnosis inference program.

The results show the possible root cause nodes on the corresponding time slice, the possible anomalous states, the possible triggering time range, and the probability of being in each anomalous state. The probabilities of the fault nodes being in different abnormal states, obtained from running the inference program, are shown in Fig. 19.

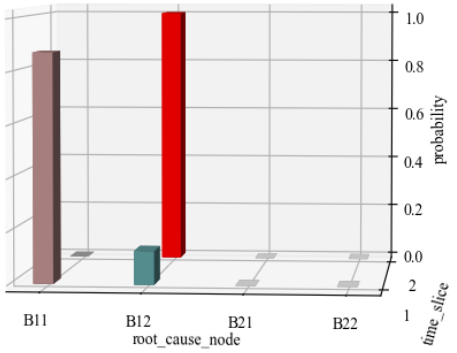

Fig. 19. Probability of abnormal state of the failure mode node.

From the reasoning process, it can be observed that the TC-DUCG takes into account the uncertainty of causal relationships between variables, temporal constraints, and the dynamic process of variable state changes. It can effectively model the complex temporal and logical dependencies between node variables in the fault propagation process. This method is suitable for diagnosing intermittent faults caused by temporal and state coupling. Furthermore, the model also exhibits good interpretability. It should be noted that the DUCG and Cubic DUCG models do not consider the time constraint of fault propagation. Furthermore, the model's inference process does not consider the dynamic change of the fault source state and the case of multiple fault sources. The TFPG model assumes that the state remains unchanged after a fault effect reaches the node and thus does not account for intermittent faults. In addition, the causal relationships between variables in the TFPG model are deterministic, which prevents effective expression of uncertainty in fault propagation.

5. Conclusion

This paper considers the intermittent nature of fault symptoms caused by the temporal and state coupling among variables. The fault symptoms only occur when certain combinations of variables are satisfied. Any changes to the variables would result in the conditions not being met, leading to the disappearance of the fault symptoms. In order to model intermittent faults caused by temporal and state coupling, a new causal model is proposed to represent the complex logical and temporal dependencies among multi-state variables. The TC-DUCG model flexibly expresses the temporal and state coupling among variables through special combinatorial gates. Additionally, a fault diagnostic reasoning method is proposed that makes full use of the temporal information and the propagation probability information of observed variables. In the inference process, the observed evidence is partitioned based on the time of variable state changes. Furthermore, time range and logical matching analysis are conducted on the evidence within the same time slice to improve the accuracy of the inference results. Finally, the effectiveness of the proposed method is validated through an illustrative example.

For future research, we plan to optimize the proposed TC-DUCG model to improve its efficiency and accuracy in dealing with intermittent faults in large-scale and complex systems. Furthermore, the specific methodology employed for the acquisition of model parameters is beyond the scope of this paper. This represents one of the points for future research.

Acknowledgment

This work was supported partially by the National Natural Science Foundation of China under grant No.62203361, the National Fund under grant No.0622-GKGJ30000030094-ZB-Z002-0, the Young Talent Fund of Association for Science and Technology in Shaanxi, the Project of National Defense Basic Research Program, National Key Scientific Research Project under grant No.MJZ2-4N21.

References

1. Bakhshi R, Kunche S, Pecht M. Intermittent failures in hardware and software. Journal of Electronic Packaging. 2014;136(1). https://doi.org/10.1115/1.4026639
2. Qi H, Ganesan S, Pecht M. No-fault-found and intermittent failures in electronic products. Microelectronics Reliability. 2008;48(5):663-74. https://doi.org/10.1016/j.microrel.2008.02.003
3. Shen Q, Qiu J, Liu G, Lv K. Intermittent fault's parameter framework and stochastic petri net based formalization model. Eksploatacja i Niezawodnosc - Maintenance and Reliability. 2016;18(2):210-7. https://doi.org/10.17531/ein.2016.2.8
4. Yuan S, Wang H, Sun X. Research on intermittent fault diagnosis of rolling bearing based on interval-valued evidence construction and possibility. Measurement. 2022;203: https://doi.org/10.1016/j.measurement.2022.111958
5. Lin L, Zhou S, Hsieh SY. Neural Network Enabled Intermittent Fault Diagnosis Under Comparison Model. IEEE Transactions on Reliability. 2023;72(3):1206-19. https://doi.org/10.1109/TR.2022.3199504
6. Qu J, Fang X, Chai Y, Tang Q, Liu J. An intermittent fault diagnosis method of analog circuits based on variational modal decomposition and adaptive dynamic density peak clustering. Soft Computing. 2022;26(17):8603-15. https://doi.org/10.1007/s00500-022-07226-1
7. Fang X, Qu J, Chai Y, Liu B. Adaptive multiscale and dual subnet convolutional auto-encoder for intermittent fault detection of analog circuits in noise environment. ISA Transactions. 2023;136:428-41. https://doi.org/10.1016/j.isatra.2022.10.031
8. Fang X, Qu J, Chai Y. Self-supervised intermittent fault detection for analog circuits guided by prior knowledge. Reliability Engineering & System Safety. 2023;233: https://doi.org/10.1016/j.ress.2023.109108.
9. Wang S, Liu Z, Jia Z, Zhao W, Li Z. Intermittent fault diagnosis for electronics-rich analog circuit systems based on multi-scale enhanced convolution transformer network with novel token fusion strategy. Expert Systems with Applications. 2024;238: https://doi.org/10.1016/j.eswa.2023.121964.
10. Zhou D, Zhao Y, Wang Z, He X, Gao M. Review on diagnosis techniques for intermittent faults in dynamic systems. IEEE Transactions on Industrial Electronics. 2019;67(3):2337-47. https://doi.org/10.1109/TIE.2019.2907500
11. Jin Y, Zhang Q, Chen Y, Lu Z, Zu T. Cascading failures modeling of electronic circuits with degradation using impedance network. Reliability Engineering & System Safety. 2023;233: https://doi.org/10.1016/j.ress.2023.109101.
12. Cui Y, Shi J, Wang Z. Fault propagation reasoning and diagnosis for computer networks using cyclic temporal constraint network model. IEEE Transactions on Systems, Man, and Cybernetics: Systems. 2016;47(8):1965-78. https://doi.org/10.1109/TSMC.2016.2583509
13. Xu J, Wang R, Liang Z, Liu P, Gao J, Wang Z. Physics-guided, data-refined fault root cause tracing framework for complex electromechanical system. Reliability Engineering & System Safety. 2023;236: https://doi.org/10.1016/j.ress.2023.109293.
14. Li W, Li H, Gu S, Chen T. Process fault diagnosis with model- and knowledge-based approaches: Advances and opportunities. Control Engineering Practice. 2020;105: https://doi.org/10.1016/j.conengprac.2020.104637.
15. Zhu P, Han J, Liu L, Zuo MJ. A stochastic approach for the analysis of fault trees with priority and gates. IEEE Transactions on Reliability. 2014;63(2):480-94. https://doi.org/10.1109/TR.2014.2313796
16. Zhu P, Han J, Liu L, Lombardi F. A stochastic approach for the analysis of dynamic fault trees with spare gates under probabilistic common cause failures. IEEE Transactions on Reliability. 2015;64(3):878-92. https://doi.org/10.1109/TR.2015.2419214
17. Cai B, Huang L, Xie M. Bayesian networks in fault diagnosis. IEEE Transactions on Industrial Informatics. 2017;13(5):2227-40. https://doi.org/10.1109/TII.2017.2695583
18. Kumari P, Bhadriraju B, Wang Q, Kwon JSI. A modified Bayesian network to handle cyclic loops in root cause diagnosis of process faults in the chemical process industry. Journal of Process Control. 2022;110:84-98. https://doi.org/10.1016/j.jprocont.2021.12.011
19. Huang W, Kou X, Zhang Y, Mi R, Yin D, Xiao W, et al. Operational failure analysis of high-speed electric multiple units: A Bayesian network-K2 algorithm-expectation maximization approach. Reliability Engineering & System Safety. 2021;205: https://doi.org/10.1016/j.ress.2020.107250
20. Zhang Q. Dynamic uncertain causality graph for knowledge representation and reasoning: Discrete DAG cases. Journal of Computer Science and Technology. 2012;27(1):1-23. https://doi.org/10.1007/s11390-012-1202-7
21. Zhang Q, Geng S. Dynamic uncertain causality graph applied to dynamic fault diagnoses of large and complex systems. IEEE Transactions on Reliability. 2015;64(3):910-27. https://doi.org/10.1109/TR.2015.2416332

22. Li L, Yue W. Dynamic uncertain causality graph based on Intuitionistic fuzzy sets and its application to root cause analysis. Applied Intelligence. 2020;50(1):241-55. https://doi.org/10.1007/s10489-019-01520-6
23. Dong C, Zhou J. A New Algorithm of Cubic Dynamic Uncertain Causality Graph for Speeding Up Temporal Causality Inference in Fault Diagnosis. IEEE Transactions on Reliability. 2023;72(2):662-77. https://doi.org/10.1109/TR.2022.3170063
24. Zhang Q, Bu X, Zhang M, Zhang Z, Hu J. Dynamic uncertain causality graph for computer-aided general clinical diagnoses with nasal obstruction as an illustration. Artificial Intelligence Review. 2021;54:27-61. https://doi.org/10.1007/s10462-020-09871-0
25. Abdelwahed S, Karsai G, Mahadevan N, Ofsthun SC. Practical implementation of diagnosis systems using timed failure propagation graph models. IEEE Transactions on Instrumentation and Measurement. 2008;58(2):240-7. https://doi.org/10.1109/TIM.2008.2005958
26. Breitfelder K, Messina D. IEEE 100: the authoritative dictionary of IEEE standards terms. Standards Information Network IEEE Press v879. 2000.
27. Zhong T, Qu J, Fang X, Li H, Wang Z. The intermittent fault diagnosis of analog circuits based on EEMD-DBN. Neurocomputing. 2021;436:74-91. https://doi.org/10.1016/j.neucom.2021.01.001
28. Dong C, Zhang Q. The cubic dynamic uncertain causality graph: A methodology for temporal process modeling and diagnostic logic inference. IEEE Transactions on Neural Networks and Learning Systems. 2020;31(10):4239-53. https://doi.org/10.1109/TNNLS.2019.2953177
29. Li Q. Analysis and Modeling Method of Hierarchical Propagation Characteristics of Electronic Equipment Faults. National University of Defense Technology; 2021.